



Article

Efficient Removal of Nonylphenol Isomers from Water by Use of Organo-Hydrotalcites

Daniel Cosano *, Dolores Esquivel , Francisco J. Romero-Salguero , César Jiménez-Sanchidrián and José Rafael Ruiz *

Departamento de Química Orgánica, Instituto Universitario de Investigación en Química Fina y Nanoquímica IUNAN, Facultad de Ciencias, Universidad de Córdoba, Campus de Rabanales, Edificio Marie Curie, E-14071 Córdoba, Spain; q12esmem@uco.es (D.E.); qo2rosaf@uco.es (F.J.R.-S.); qo1jjsac@uco.es (C.J.-S.)

* Correspondence: q92cohid@uco.es (D.C.); qo1ruarj@uco.es (J.R.R.); Tel.: +34-957-218623 (D.C.); +34-957-218638 (J.R.R.)

Abstract: The presence of potent organic endocrine-disrupting chemicals (EDCs) in natural aquifers can have adverse impacts on public health and the environment. 4-nonylphenol, one such EDC, can be efficiently removed from water by adsorption onto a clayey material. In this work, we created an effective sorbent for this purpose by using co-precipitation and subsequent ion-exchange to intercalate the organic anion deoxycholate into a Mg/Al hydrotalcite. Intercalating deoxycholate ions increased the organophilicity of the hydrotalcite surface. The solid was used to adsorb 4-nonylphenol at different pollutant concentrations and temperatures. The adsorption process was subjected to a kinetic study. Based on the results, the EDC was adsorbed by chemisorption. In addition, based on the equilibrium isotherms used for the process, the Freundlich model was the most accurate in reproducing the adsorption of 4-nonylphenol onto deoxycholate-intercalated hydrotalcite.

Keywords: hydrotalcite; deoxycholate; adsorption; nonylphenol removal



Citation: Cosano, D.; Esquivel, D.; Romero-Salguero, F.J.; Jiménez-Sanchidrián, C.; Ruiz, J.R. Efficient Removal of Nonylphenol Isomers from Water by Use of Organo-Hydrotalcites. *Int. J. Environ. Res. Public Health* **2022**, *19*, 7214. <https://doi.org/10.3390/ijerph19127214>

Academic Editors:
Panagiotis Karanis, Layla Ben Ayed,
Eleni Golomazou, Patrick Scheid,
Ourania Tzoraki, Anna Lass and
Muhammad Shahid Iqbal

Received: 5 April 2022
Accepted: 8 June 2022
Published: 12 June 2022

Publisher's Note: MDPI stays neutral with regard to jurisdictional claims in published maps and institutional affiliations.



Copyright: © 2022 by the authors. Licensee MDPI, Basel, Switzerland. This article is an open access article distributed under the terms and conditions of the Creative Commons Attribution (CC BY) license (<https://creativecommons.org/licenses/by/4.0/>).

1. Introduction

An increasing number of aquifers are being contaminated with endocrine-disrupting chemicals (EDCs). Although EDC concentrations in water are usually very low (typically in the microgram-per-liter or nanogram-per-liter range [1,2]), they can have deleterious effects on human health, such as endocrine disorders or abnormal organ development [3–5]. The presence of EDCs in water usually results from their use as additives in detergents, perfumes, and creams, among other products. Because most wastewater purification plants fail to remove the typically low concentrations of EDCs [6], these organic compounds must be eliminated with alternative procedures such as chemical oxidation [7] or physisorption [8–11]. Worthy of note is that among EDCs are nonylphenols, which typically comprise a mixture of chain and position isomers (NPhOH) and linear polyphenol at position 4 on an aromatic ring (4-NPhOH; Figure 1). These compounds, and short-chain ethoxylated nonylphenols, are usually degradation products of long-chain ethoxylated nonylphenols, which are surface-active and used in a variety of detergent, pesticide, packaging plastic, and cosmetic formulations. Upon discharge into the environment, these products are microbially converted into nonylphenols (particularly 4-NPhOH, which is the most widely used by the detergent industry [12]).

One of the main reasons for removing nonylphenols is their usually high concentration found in sewage sludge—a result of the ease with which they can be adsorbed onto solids such as sediments, sludge, and soil. Using sewage sludge in agriculture [13] can lead to contamination not only of soil, crops, and living organisms, but also of underground waters by leaching and ground waters by run-off [14]. Due to the high affinity of nonylphenol for some solids, a variety of materials have been used to remove nonylphenols from

water by adsorption, including mica [8], organic polymers [9,15], modified clays [16], iron oxides [17,18], carbon nanotubes [19], and graphene oxides [20,21].

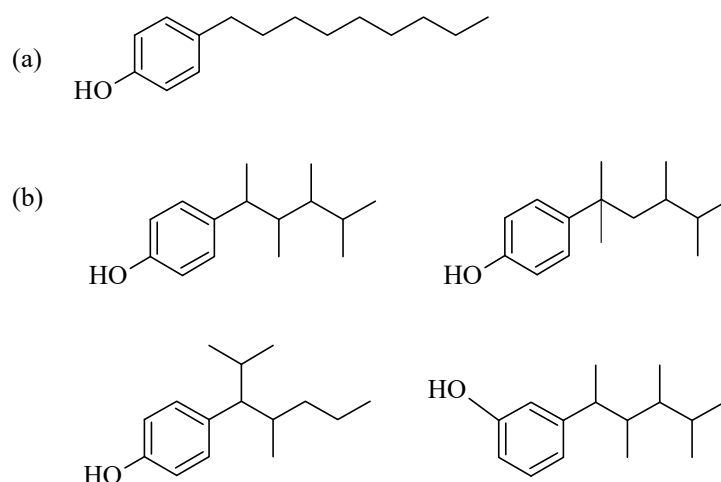


Figure 1. Chemical structure of 4-nonylphenol (4-NPhOH) (a); chain and position isomers of nonylphenol (b).

Hydrotalcites, also known as “anionic clays” or “layered double hydroxides”, are widely used as sorbents for both organic and inorganic water pollutants [22–25]. Hydrotalcite, the parent compound, is a natural mineral of the formula $Mg_6Al_2(CO_3)_2(OH)_2 \cdot 6H_2O$, where magnesium and aluminum can be substituted by another divalent or trivalent metal, respectively, provided its ionic radius is similar to that of Mg or Al, respectively. In addition, carbonate ion can be substituted by a wide range of organic and inorganic anions [26,27]. The general formula for a hydrotalcite is thus $[M(II)_{1-x}M(III)_x(OH)_2]^{x+}[A_{n/x}]^{n-} \cdot mH_2O$, where $M(II)$ is a divalent metal, $M(III)$ is a trivalent one, A is an anion, x is the atomic ratio $M(III)/[M(II) + M(III)]$, and m is the number of water molecules present in the interlayer region. Usually, x can range from 0.2 with a metal ratio of 4 to 0.33 with 1 of 2.

Structurally, hydrotalcites are similar to the natural magnesium oxide brucite $[Mg(OH)_2]$. Thus, they consist of positively charged octahedral layers of metal hydroxides intercalated with anions that offset the positive charge. The interlayer region can additionally accommodate water molecules forming hydrogen bonds with the anion and/or metal layers.

Our research group previously used hydrotalcites as sorbents for cyanide [28]. However, despite their wide use as sorbents, these solids have very rarely, to our knowledge, been used to remove nonylphenol [29,30]. In this work, a hydrotalcite intercalated with an organic anion (deoxycholate) was, for the first time, used as a sorbent for nonylphenol in water. Organo-HT appears to be a suitable alternative to the adsorption, with calcined hydrotalcites easing the reusability of the material.

2. Materials and Methods

2.1. Materials

Sodium deoxycholate (DCH) and nonylphenol (Figure 1) were Sigma–Aldrich (USA) ref. D6750 and 290858. The metal salts $[Mg(NO_3)_2 \cdot 6H_2O]$, ref. 141402; $[Al(NO_3)_3 \cdot 9H_2O]$, ref. 131099] and sodium hydroxide (NaOH, ref. 141687) were supplied by Panreac.

2.2. Preparation of the Sorbent

The sorbent used was a hydrotalcite with a Mg/Al ratio of 2.5 and containing intercalated deoxycholate anion to counter-charge in the metal layers. The solid was obtained in two steps. The first involved using a co-precipitation method to synthesize a Mg/Al hydrotalcite with nitrate as an interlayer anion, and the second involved exchanging the nitrate with deoxycholate ion by using a microwave-assisted procedure previously developed

by our group [31]. Compositional and structural properties of the resulting hydrotalcite, designated HT-DSC, are summarized in Table 1.

Table 1. Compositional and structural properties determined for HT-DSC [31].

| Solid | Mg/Al _{Ther} | Mg/Al _{exp} ^a | A (nm) | C (nm) |
|--------------|-----------------------|-----------------------------------|--------|--------|
| Hydrotalcite | 2.5 | 2.41 | 0.305 | 9.810 |

^a Mg/Al_{exp} ratio was calculated by inductively coupled plasma mass spectrometry (ICP-MS).

2.3. Adsorption Tests

The adsorption of 4-nonylphenol (4-NPhOH) onto deoxycholate-intercalated hydrotalcite was examined by using solutions containing variable concentrations of adsorbate at their natural pH at room temperature. Each solution was prepared by adding an appropriate amount of 4-NPhOH to a 250 mL flask containing 25 mL of distilled water and then 100 mg of HT-DSC under continuous stirring, with periodic withdrawal of samples to quantify the amount of 4-NPhOH remaining in solution by gas chromatography–mass spectrometry (GC–MS). Once adsorption equilibrium was reached, stirring of the solution was continued for a few hours before it was stopped and the solid filtered off for GC–MS analysis on a Varian 3900 chromatograph coupled to a Varian Saturn 2100T mass spectrometer.

2.4. Kinetic Tests

One of the central aspects of an adsorption process is its kinetics. The kinetics of 4-nonylphenol adsorption onto the hydrotalcite was examined by using the previous 25 mL solution under the conditions described in Section 2.2. The amount of 4-NPhOH adsorbed onto the solid was calculated from the equation $q_t = ([NPhOH]_0 - [NPhOH]_t/m) \cdot V$, where q_t is the adsorption capacity of the hydrotalcite at time t in μg 4-NPhOH/g hydrotalcite; V is the volume of solution in mL; and $[NPhOH]_0$ and $[NPhOH]_t$ are the initial concentrations of adsorbate at time t in ppm. The optimum amounts of 4-NPhOH and sorbent, and the optimum temperature, to be used were all determined by testing.

The isotherms for nonylphenol adsorption onto the hydrotalcite were obtained with the batch equilibrium method, changing the concentration of nonylphenol and keeping all other variables constant over a long enough period for equilibrium to be reached.

3. Results and Discussion

3.1. Adsorption Tests

Figure 2 shows the time course of the 4-NPhOH concentration in the adsorption tests. Equilibrium was reached after about 60 min. The curve initially exhibited a very steep slope owing to the large number of free adsorption sites present in the hydrotalcite. However, the rate of the process decreased as such sites were gradually occupied by the adsorbate until equilibrium was reached. As can be seen from Figure 2, the lower the initial concentration of nonylphenol, the lower at which the system equilibrated. This was a logical result as the amount of sorbent used was identical in all tests, so the ratio of sorbent sites to nonylphenol molecules increased with increasing concentration of adsorbate.

The initially fast adsorption of 4-NPhOH was a result of the high capacity of its molecules to interact with deoxycholate ions on the HT-DSC surface. Moreover, the decrease in adsorption rate apparent from Figure 2 must have resulted from 4-NPhOH diffusing over the interlayer region in the sorbent. Therefore, 4-NPhOH was adsorbed onto the outer surface of the hydrotalcite at a high rate. After the surface saturated with adsorbate, excess 4-NPhOH started to diffuse over the hydrotalcite pore network and was adsorbed on the interlayer region [32], all at a much lower rate than in the previous process. As can be seen from the curves of Figure 2, the initial concentration of 4-NPhOH was strongly influential on its adsorption. Increasing the number of 4-NPhOH molecules in

the solution increased the rate of mass transfer—and hence that of adsorption onto the hydrotalcite surface [32]—and the amount of nonylphenol adsorbed as a result.

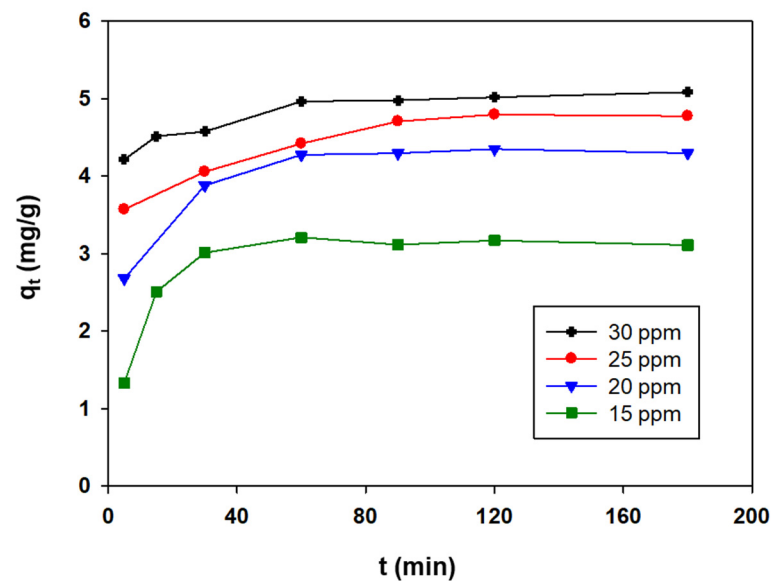


Figure 2. Influence of the initial concentration on the adsorption of 4-NPhOH on HT-DSC (experimental conditions: 25 mL of solution; 100 mg of adsorbent; 24 °C).

Several kinetics models, represented below, were used to illustrate the 4-NPhOH adsorption into the HT-DSC (see Figure 3 and Figures S1–S3) [33,34]. It is essential to be wary that a relatively high R^2 value for a specific kinetic model does not incidentally mean that this model is the only descriptive model [34–37].

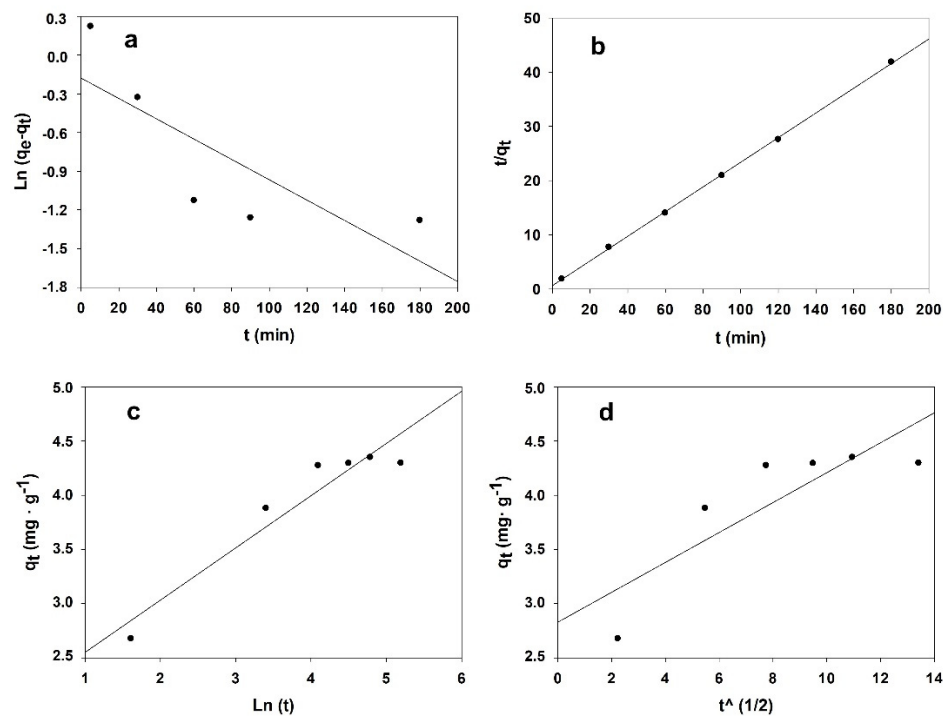


Figure 3. Kinetic models for 20 ppm concentration: (a) pseudo-first order kinetic model; (b) pseudo-second order kinetic model; (c) Elovich kinetic model; (d) and interparticle diffusion kinetic model.

The adsorption process was examined in the light of a pseudo-first order model and a pseudo-second order model. The former uses Equation 1 to represent the rate of adsorption of a liquid phase onto a solid phase.

$$\log (q_e - q_t) = \log q_e - k_1 \cdot t, \quad (1)$$

where q_e and q_t are the amounts of 4-NPhOH adsorbed per gram of hydrotalcite at equilibrium and time t , respectively, and k_1 is the pseudo-first-order kinetic constant for the process.

The pseudo-second order model is based on Equation (2) and assumes that the adsorbate is adsorbed by chemisorption.

$$t/q_t = (1/k_2 \cdot q_e^2) + (t/q_e), \quad (2)$$

where q_e and q_t have the same meaning as in Equation (1), and k_2 is the pseudo-second order rate constant for the process.

Table 2 shows the kinetic parameters and correlation coefficients obtained within each model. As can be seen, the pseudo-second order model provided better correlation. This suggests that, as shown below, 4-NPhOH was chemisorbed onto the hydrophobic, hydrocarbon portion of deoxycholate on the outer surface of the hydrotalcite.

Table 2. Kinetics parameters and correlation coefficients for the sorbent.

| T (K) | | Pseudo-First Order | | Pseudo-Second Order | | Elovich | | Intra-Particle Diffusion | | |
|-------|-----|--------------------|----------------|---------------------|----------------|----------------|-------|--------------------------|--------------------|-------|
| | | R ² | K ₁ | R ² | K ₂ | R ² | B | R ² | K _{Intra} | c |
| 30 | 298 | 0.824 | 0.010 | 0.938 | 0.169 | 0.960 | 3.917 | 0.881 | 0.077 | 4.176 |
| 25 | 298 | 0.962 | 0.009 | 0.980 | 0.154 | 0.961 | 2.699 | 0.910 | 0.117 | 3.426 |
| 20 | 298 | 0.921 | 0.031 | 0.993 | 0.148 | 0.910 | 2.075 | 0.712 | 0.138 | 2.828 |
| 15 | 298 | 0.893 | 0.051 | 0.957 | 0.132 | 0.802 | 1.962 | 0.559 | 0.127 | 1.810 |

The kinetic study was expanded by using the Elovich equation, which is typically used to describe the kinetics of a pseudo-second order process when its steady-state energy is not constant and the adsorbate is chemically adsorbed:

$$q_t = (\text{Ln } h_b + \text{Ln } t)/B, \quad (3)$$

where h_b and B are Elovich's constants.

As can be inferred from Figure 3c, nonylphenol was adsorbed in two steps, namely: a very fast step where most of the adsorbate was adsorbed onto the hydrotalcite, followed by a slower step where the remainder adsorbate was incorporated onto the sorbent.

As confirmed by the intraparticle diffusion model, the adsorption process was chemical in nature. The hypothesis of intraparticle diffusion within pores in a sorbent particle assumes that the adsorbate is carried through the inner structure of the sorbent pore network by diffusion. Intraparticle diffusion conforms to Equation 4, which relates to specific adsorption to the square root of time.

$$q_t = (k_{\text{intra}} \cdot t^{0.5}) + C, \quad (4)$$

where C is the concentration of adsorbate initially adsorbed.

We also examined the influence of temperature on the adsorption process. Some authors have shown that temperature strongly influences the adsorption of organic compounds onto various types of solid sorbents [9,19,35,38]. In this work, we examined the adsorption of 4-NPhOH onto HT-DSC at 298, 313, and 333 K. The rate of 4-NPhOH adsorption onto the hydrotalcite was found to increase with increasing temperature (results not

shown); therefore, the process was endothermic. The activation energy was calculated from the Arrhenius equation in logarithmic form:

$$\ln k_2 = \ln A - (E_a/RT), \quad (5)$$

A plot of $\ln k_2$ against the reciprocal temperature (Figure 4) was a straight line with a very high correlation coefficient that allowed the Arrhenius constant and activation energy to be easily calculated. The latter was 20.19 kJ/mol. This shows that the adsorption process was by chemical adsorption [39].

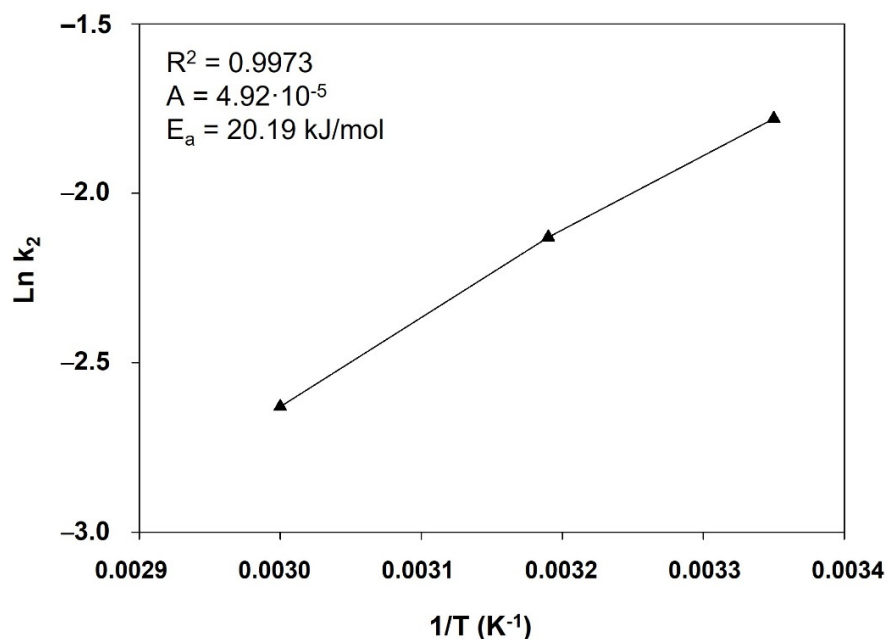


Figure 4. Variation of $\ln k_2$ versus the inverse of temperature.

The adsorption isotherm was constructed from the results obtained at 298 K. The experimental data were fitted by using the three most common models for this purpose, which are based on the Langmuir, Freundlich, and Temkin isotherms (see Figure 5) [34,40].

The Langmuir isotherm is a theoretical model accurately representing monolayer adsorption onto a uniform surface containing a finite number of specific adsorption sites, where the adsorbate and sorbent interact to a negligible extent. Mathematically, the Langmuir isotherm is defined by

$$C_{eq}/C_{ads} = (1/bQ) + (C_{eq}/Q), \quad (6)$$

where C_{eq} is the equilibrium adsorption concentration of 4-NPhOH (mg/L), Q is the amount of 4-NPhOH adsorbed per unit mass of sorbent (mg/g) with monolayer coverage, C_{ads} is the Q value at equilibrium (mg/g), and b is a constant related to the affinity of binding sites.

The Freundlich model is based on an empirical equation assuming energy non-uniformity among specific adsorption sites, and exposes a consistently exponential distribution of active sites over a non-uniform surface:

$$C_{ads} = K_f \cdot C_{eq}^{1/n}, \quad (7)$$

Or, in logarithmic form,

$$\log C_{ads} = \log K_f + (1/n) \cdot \log C_{eq}, \quad (8)$$

where K_f and n are two Freundlich temperature-dependent constants.

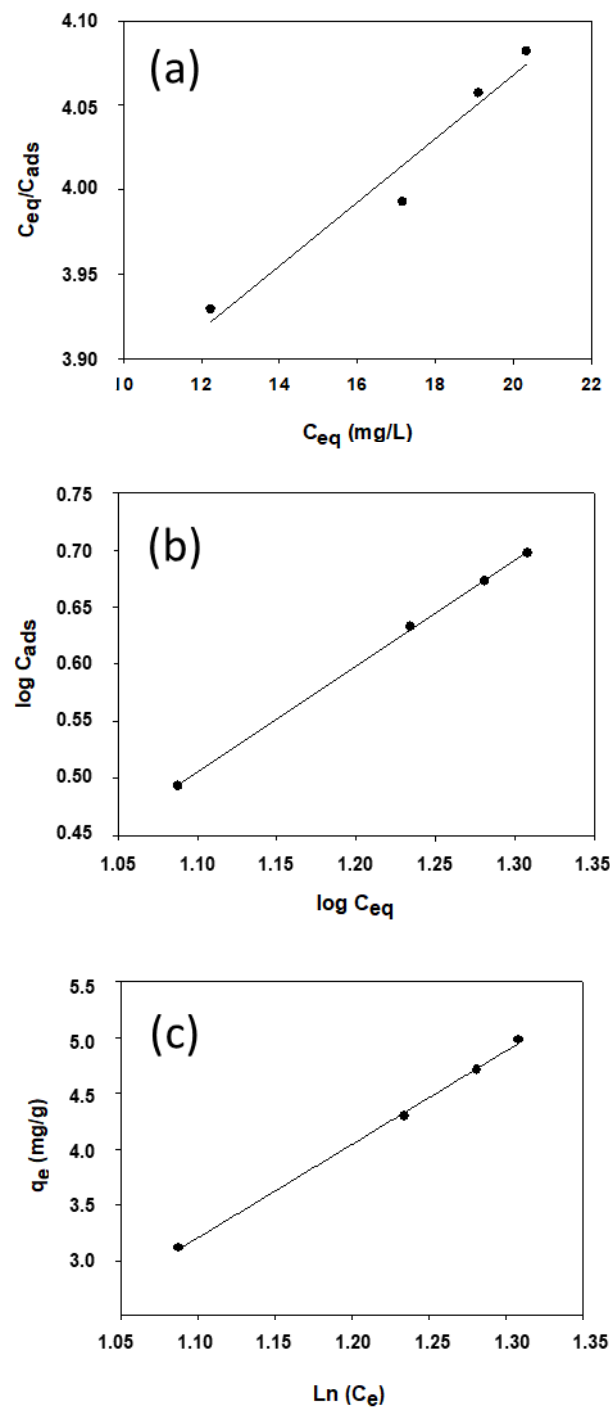


Figure 5. Langmuir (a), Freundlich (b), and Temkin (c) plots for 4-NPhOH adsorption on the HT-DSC.

The Temkin model assumes a uniform distribution of binding energies and introduces constants depending on the initial heat of adsorption. It also assumes such heat to decrease linearly with increasing coverage. The model is based on the following equation:

$$q_e = RT \cdot (\ln K_T + \ln C_e) / b_T, \quad (9)$$

where K_T and b_T are Temkin's equilibrium binding constant (L/g) and adsorption heat constant, respectively.

Table 3 shows the figures of merit of each type of isotherm and its correlation coefficients (R^2). The results suggest that the Freundlich model describes the sorption equilibrium

more accurately than the Langmuir and Temkin models. Thus, 4-NPhOH adsorption on the hydrotalcite does not result in complete coverage of the solid surface; the adsorption energy decreases exponentially as 4-NPhOH is adsorbed onto the solid. As can be seen from Table 3, the Temkin model exhibited high correlation, which is unsurprising since it assumes the adsorption energy to decrease linearly with increasing adsorption of the adsorbate—as it did here based on the results obtained with the Freundlich model. In general, the hydrophobic interaction was the main sorption mechanism when both organic pollutants and the surface of materials are hydrophobic.

Table 3. Isotherm adsorption parameters for the different models.

| | | | |
|-------------------|---------------|-----------------------|---------------|
| Langmuir | Q = 53.19 | $b = 5 \cdot 10^{-3}$ | $R^2 = 0.956$ |
| Freundlich | $K_F = 0.306$ | n = 1.079 | $R^2 = 0.999$ |
| Temkin | $K_T = 0.488$ | $b_T = 2.919$ | $R^2 = 0.998$ |

R_L is the dimensionless constant that predicts whether the adsorption system is efficient or not, defined by Weber and Chakravorti [41] as:

$$R_L = 1/(1 + K_L \cdot C_0), \quad (10)$$

where K_L is the constant of Langmuir and C_0 is initial 4-NPhOH concentration ($\text{mg} \cdot \text{g}^{-1}$). The parameter R_L indicates the shape of isotherm, where: $0 < R_L < 1$ the adsorption is favorable, $R_L > 1$ the adsorption is unfavorable, $R_L = 1$ is linear adsorption and $R_L = 0$ is irreversible [42,43]. For 4-NPhOH, a value of $R_L = 0.3378$ is obtained, which means the adsorption process is favorable.

3.2. Reusability of the Adsorbent

Three reuses were carried with HT-DSC as adsorbent with a 4-NPhOH concentration of 30 ppm. Figure 6 shows the adsorption cycles performed at 30 min. As can be seen, the recyclability of HT-DSC is effective, showing an adsorption capacity similar to that obtained by the fresh adsorbent. Only a 10% decrease in adsorption capacity was observed for each recycle. A washing step with CH_3OH was carried out between each reuse to desorb the adsorbed 4-NPhOH on the HT-DSC. It is known that the hydrophobic interaction between the aromatic ring of 4-NPhOH and the hydrocarbon portion of deoxycholate molecules on the material produces weak bonds, which are easily broken out during the washing step with CH_3OH .

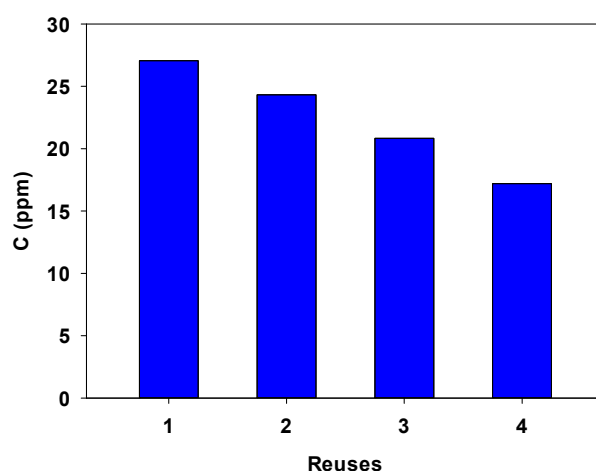


Figure 6. Reuse of HT-DSC for the adsorption of 4-NPhOH. Experimental conditions: 25 mL of adsorbate solution, 100 mg of sorbent, and 22 °C. Where “1” is fresh material.

4. Conclusions

In this work, we used a hydrotalcite intercalated with deoxycholate anion as sorbent to remove the organic pollutant nonylphenol from water. Although the adsorption rate was influenced by the pollutant concentration, the adsorption process reached equilibrium after about 60 min. The ratio of the number of sorbent sites to that of nonylphenol molecules increased with decreasing concentration of pollutant in the aqueous solution. The pollutant was very rapidly adsorbed onto the outer surface of the hydrotalcite. 4-NPhOH was chemisorbed onto the hydrophobic, hydrocarbon portion of deoxycholate on the outer surface of the hydrotalcite. Once the outer surface saturated, however, the adsorbate diffused over the pore network of the solid and was adsorbed on the interlayer region, albeit more slowly than it was on the solid surface. Nonylphenol adsorption onto the hydrotalcite was found to be a pseudo-second order process. The results suggest that the Freundlich model describes the sorption equilibrium proving a chemisorption interaction. Finally, for 4-NPhOH, a value of R_L means that the adsorption process is favorable.

Supplementary Materials: The following supporting information can be downloaded at: <https://www.mdpi.com/article/10.3390/ijerph19127214/s1>, Figure S1: Kinetic models for 15 ppm concentration: (a) pseudo-first-order kinetic model, (b) pseudo-second-order kinetic model, (c) Elovich kinetic model, (d) and interparticle diffusion kinetic model. Figure S2: Kinetic models for 25 ppm concentration: (a) pseudo-first-order kinetic model, (b) pseudo-second-order kinetic model, (c) Elovich kinetic model, (d) and interparticle diffusion kinetic model. Figure S3: Kinetic models for 30 ppm concentration: (a) pseudo-first-order kinetic model, (b) pseudo-second-order kinetic model, (c) Elovich kinetic model, (d) and interparticle diffusion kinetic model.

Author Contributions: D.C. and J.R.R. carried out the research sampling and processing. D.C. and J.R.R. performed the data analysis and interpretation. Critical review of the manuscript was performed by D.E., F.J.R.-S., and C.J.-S. All authors have read and agreed to the published version of the manuscript.

Funding: This research was funded by Spanish Ministry of Education and Science (Project RTI2018-101611-B-100).

Institutional Review Board Statement: Not applicable.

Informed Consent Statement: Not applicable.

Data Availability Statement: The authors declare that the manuscript is original, has not been submitted to or published in any other journal, and the data in the manuscript is real.

Acknowledgments: The authors gratefully acknowledge the Spanish Ministry of Education and Science, D. C. acknowledges to 2014–2020 Social European Fund program of Andalusia (DOC_01376, FEDER).

Conflicts of Interest: The authors declare no conflict of interest.

References

1. Ruhí, A.; Acuña, V.; Barceló, D.; Huerta, B.; Mor, J.R.; Rodríguez-Mozaz, S.; Sabater, S. Bioaccumulation and trophic magnification of pharmaceuticals and endocrine disruptors in a Mediterranean river food web. *Sci. Total Environ.* **2016**, *540*, 250–259. [[CrossRef](#)] [[PubMed](#)]
2. Koumaki, E.; Mamais, D.; Noutsopoulos, C. Assessment of the environmental fate of endocrine disrupting chemicals in rivers. *Sci. Total Environ.* **2018**, *628–629*, 947–958. [[CrossRef](#)] [[PubMed](#)]
3. Campbell, C.G.; Borglin, S.E.; Green, F.B.; Grayson, A.; Wozel, E.; Stringfellow, W.T. Biologically directed environmental monitoring, fate, and transport of estrogenic endocrine disrupting compounds in water: A review. *Chemosphere* **2006**, *65*, 1265–1280. [[CrossRef](#)] [[PubMed](#)]
4. Valbonesi, P.; Profita, M.; Vasumini, I.; Fabbri, E. Contaminants of emerging concern in drinking water: Quality assessment by combining chemical and biological analysis. *Sci. Total Environ.* **2021**, *758*, 143624. [[CrossRef](#)] [[PubMed](#)]
5. Park, H.; Kim, K. Urinary levels of 4-nonylphenol and 4-t-octylphenol in a representative sample of the Korean adult population. *Int. J. Environ. Res. Public Health* **2017**, *14*, 932. [[CrossRef](#)] [[PubMed](#)]

6. Rott, E.; Kuch, B.; Lange, C.; Richter, P.; Kugele, A.; Minke, R. Removal of emerging contaminants and estrogenic activity from wastewater treatment plant effluent with UV/chlorine and UV/H₂O₂ advanced oxidation treatment at pilot scale. *Int. J. Environ. Res. Public Health* **2018**, *15*, 935. [[CrossRef](#)]
7. Capodaglio, A.G. High-energy oxidation process: An efficient alternative for wastewater organic contaminants removal. *Clean Technol. Environ. Policy* **2017**, *19*, 1995–2006. [[CrossRef](#)]
8. Martín, J.; Orta, M. del M.; Medina-Carrasco, S.; Santos, J.L.; Aparicio, I.; Alonso, E. Removal of priority and emerging pollutants from aqueous media by adsorption onto synthetic organo-functionalized high-charge swelling micas. *Environ. Res.* **2018**, *164*, 488–494. [[CrossRef](#)]
9. Tang, P.; Sun, Q.; Suo, Z.; Zhao, L.; Yang, H.; Xiong, X.; Pu, H.; Gan, N.; Li, H. Rapid and efficient removal of estrogenic pollutants from water by using beta- and gamma-cyclodextrin polymers. *Chem. Eng. J.* **2018**, *344*, 514–523. [[CrossRef](#)]
10. Hu, S.; Xu, D.; Kong, X.; Gong, J.; Yang, Y.; Ran, Y.; Mao, J. Effect of the structure and micropore of activated and oxidized black carbon on the sorption and desorption of nonylphenol. *Sci. Total Environ.* **2021**, *761*, 144191. [[CrossRef](#)]
11. Koumaki, E.; Noutsopoulos, C.; Mamais, D.; Fragkiskatos, G.; Andreadakis, A. Fate of Emerging Contaminants in High-Rate Activated Sludge Systems. *Int. J. Environ. Res. Public Health* **2021**, *18*, 400. [[CrossRef](#)] [[PubMed](#)]
12. Langford, K.H.; Lester, J.N. Fate and behavior of endocrine disruptors in wastewater treatment processes. In *Endocrine Disruptors in Wastewater and Sludge Treatment Processes*; CRC Press: Boca Raton, FL, USA, 2002; pp. 64–68.
13. Aparicio, I.; Santos, J.L.; Alonso, E. Limitation of the concentration of organic pollutants in sewage sludge for agricultural purposes: A case study in South Spain. *Waste Manag.* **2009**, *29*, 1747–1753. [[CrossRef](#)] [[PubMed](#)]
14. Ding, J.; Cheng, Y.; Hua, Z.; Yuan, C.; Wang, X. The effect of dissolved organic matter (DOM) on the release and distribution of endocrine-disrupting chemicals (EDCS) from sediment under hydrodynamic forces, a case study of Bisphenol A (BPA) and nonylphenol (NP). *Int. J. Environ. Res. Public Health* **2019**, *16*, 1724. [[CrossRef](#)] [[PubMed](#)]
15. Yu, Y.; Mo, W.Y.; Luukkonen, T. Adsorption behaviour and interaction of organic micropollutants with nano and microplastics—A review. *Sci. Total Environ.* **2021**, *797*, 149140. [[CrossRef](#)]
16. Sasai, R.; Sugiyama, D.; Takahashi, S.; Tong, Z.; Shichi, T.; Itoh, H.; Takagi, K. The removal and photodecomposition of n-nonylphenol using hydrophobic clay incorporated with copper-phthalocyanine in aqueous media. *J. Photochem. Photobiol. A Chem.* **2003**, *155*, 223–229. [[CrossRef](#)]
17. Al-Ahmari, S.D.; Watson, K.; Fong, B.N.; Ruyonga, R.M.; Ali, H. Adsorption kinetics of 4-n-nonylphenol on hematite and goethite. *J. Environ. Chem. Eng.* **2018**, *6*, 4030–4036. [[CrossRef](#)]
18. Cheng, Q.; Jiang, H.; Jin, Z.; Jiang, Y.; Hui, C.; Xu, L.; Zhao, Y.; Du, L. Effects of Fe₂O₃ nanoparticles on extracellular polymeric substances and nonylphenol degradation in river sediment. *Sci. Total Environ.* **2021**, *770*, 145210. [[CrossRef](#)]
19. Dai, Y.-D.; Shah, K.J.; Huang, C.P.; Kim, H.; Chiang, P.-C. Adsorption of Nonylphenol to Multi-Walled Carbon Nanotubes: Kinetics and Isotherm Study. *Appl. Sci.* **2018**, *8*, 2295. [[CrossRef](#)]
20. You, X.; He, M.; Cao, X.; Wang, P.; Wang, J.; Li, L. Molecular dynamics simulations of removal of nonylphenol pollutants by graphene oxide: Experimental study and modelling. *Appl. Surf. Sci.* **2019**, *475*, 621–626. [[CrossRef](#)]
21. Catherine, H.N.; Ou, M.H.; Manu, B.; Shih, Y.H. Adsorption mechanism of emerging and conventional phenolic compounds on graphene oxide nanoflakes in water. *Sci. Total Environ.* **2018**, *635*, 629–638. [[CrossRef](#)]
22. Zubair, M.; Daud, M.; McKay, G.; Shehzad, F.; Al-Harathi, M.A. Recent progress in layered double hydroxides (LDH)-containing hybrids as adsorbents for water remediation. *Appl. Clay Sci.* **2017**, *143*, 279–292. [[CrossRef](#)]
23. He, W.; Ai, K.; Ren, X.; Wang, S.; Lu, L. Inorganic layered ion-exchangers for decontamination of toxic metal ions in aquatic systems. *J. Mater. Chem. A* **2017**, *5*, 19593–19606. [[CrossRef](#)]
24. Theiss, F.L.; Couperthwaite, S.J.; Ayoko, G.A.; Frost, R.L. A review of the removal of anions and oxyanions of the halogen elements from aqueous solution by layered double hydroxides. *J. Colloid Interface Sci.* **2014**, *417*, 356–368. [[CrossRef](#)] [[PubMed](#)]
25. Goh, K.; Lim, T.; Dong, Z. Application of layered double hydroxides for removal of oxyanions: A review. *Water Res.* **2008**, *42*, 1343–1368. [[CrossRef](#)] [[PubMed](#)]
26. Tian, R.; Liang, R.; Wei, M.; Evans, D.G.; Duan, X. Applications of layered double hydroxide materials: Recent advances and perspective. In *50 Years of Structure and Bonding—The Anniversary Volume*; Springer: Berlin/Heidelberg, Germany, 2016; pp. 65–84.
27. Li, F.; Duan, X. Applications of Layered Double Hydroxides. In *Layered Double Hydroxides*; Duan, X., Evans, D.G., Eds.; Springer: Berlin/Heidelberg, Germany, 2006; pp. 193–223. ISBN 978-3-540-32495-9.
28. Cosano, D.; Esquinas, C.; Jiménez-Sanchidrián, C.; Ruiz, J.R. Use of Raman spectroscopy to assess the efficiency of MgAl mixed oxides in removing cyanide from aqueous solutions. *Appl. Surf. Sci.* **2016**, *364*, 428–433. [[CrossRef](#)]
29. Kostura, B.; Radim, Š.; Plachá, D.; Kukutschová, J.; Matýšek, D. Mg–Al–CO₃ hydrotalcite removal of persistent organic disruptor—Nonylphenol from aqueous solutions. *Appl. Clay Sci.* **2015**, *114*, 234–238. [[CrossRef](#)]
30. Zhou, Q.; Lei, M.; Li, J.; Zhao, K.; Liu, Y. Sensitive determination of bisphenol A, 4-nonylphenol and 4-octylphenol by magnetic solid phase extraction with Fe@MgAl-LDH magnetic nanoparticles from environmental water samples. *Sep. Purif. Technol.* **2017**, *182*, 78–86. [[CrossRef](#)]
31. Cosano, D.; Esquivel, D.; Romero, F.J.; Jiménez-Sanchidrián, C.; Ruiz, J.R. Microwave-assisted synthesis of hybrid organo-layered double hydroxides containing cholate and deoxycholate. *Mater. Chem. Phys.* **2019**, *225*, 28–33. [[CrossRef](#)]
32. Hameed, B.H. Equilibrium and kinetics studies of 2, 4, 6-trichlorophenol adsorption onto activated clay. *Colloids Surfaces A Physicochem. Eng. Asp.* **2007**, *307*, 45–52. [[CrossRef](#)]

33. Dinari, M.; Neamati, S. Surface modified layered double hydroxide/polyaniline nanocomposites: Synthesis, characterization and Pb²⁺ removal. *Colloids Surfaces A Physicochem. Eng. Asp.* **2020**, *589*, 124438. [[CrossRef](#)]
34. Limousin, G.; Gaudet, J.P.; Charlet, L.; Sznknect, S.; Barthès, V.; Krimissa, M. Sorption isotherms: A review on physical bases, modeling and measurement. *Appl. Geochem.* **2007**, *22*, 249–275. [[CrossRef](#)]
35. Ho, Y.S.; Ng, J.C.Y.; McKay, G. Kinetics of pollutant sorption by biosorbents: Review. *Sep. Purif. Methods* **2000**, *29*, 189–232. [[CrossRef](#)]
36. Pan, X.; Zhang, M.; Liu, H.; Ouyang, S.; Ding, N.; Zhang, P. Adsorption behavior and mechanism of acid orange 7 and methylene blue on self-assembled three-dimensional MgAl layered double hydroxide: Experimental and DFT investigation. *Appl. Surf. Sci.* **2020**, *522*, 146370. [[CrossRef](#)]
37. Zhang, C.; Yang, S.; Chen, H.; He, H.; Sun, C. Adsorption behavior and mechanism of reactive brilliant red X-3B in aqueous solution over three kinds of hydrotalcite-like LDHs. *Appl. Surf. Sci.* **2014**, *301*, 329–337. [[CrossRef](#)]
38. Yu, S.; Wang, X.; Chen, Z.; Wang, J.; Wang, S.; Hayat, T.; Wang, X. Layered double hydroxide intercalated with aromatic acid anions for the efficient capture of aniline from aqueous solution. *J. Hazard. Mater.* **2017**, *321*, 111–120. [[CrossRef](#)]
39. Zheng, L.; Dang, Z.; Yi, X.; Zhang, H. Equilibrium and kinetic studies of adsorption of Cd(II) from aqueous solution using modified corn stalk. *J. Hazard. Mater.* **2010**, *176*, 650–656. [[CrossRef](#)] [[PubMed](#)]
40. Dinari, M.; Shirani, M.A.; Maleki, M.H.; Tabatabaeian, R. Green cross-linked bionanocomposite of magnetic layered double hydroxide/guar gum polymer as an efficient adsorbent of Cr(VI) from aqueous solution. *Carbohydr. Polym.* **2020**, *236*, 116070. [[CrossRef](#)]
41. Weber, T.W.; Chakravori, R. Pore and Solid Diffusion Models for Fixed-Bed Adsorbers. *AIChE J.* **1974**, *20*, 222–238. [[CrossRef](#)]
42. Tan, I.A.W.; Ahmad, A.L.; Hameed, B.H. Adsorption isotherms, kinetics, thermodynamics and desorption studies of 2,4,6-trichlorophenol on oil palm empty fruit bunch-based activated carbon. *J. Hazard. Mater.* **2009**, *164*, 473–482. [[CrossRef](#)]
43. Vadivelan, V.; Kumar, K.V. Equilibrium, kinetics, mechanism, and process design for the sorption of methylene blue onto rice husk. *J. Colloid Interface Sci.* **2005**, *286*, 90–100. [[CrossRef](#)]